COMPARISON OF CONNEXIN32 EXPRESSION AND FUNCTION BETWEEN MCF10A NORMAL BREAST AND MDA-MB-231 BREAST CANCER CELL LINES

A Thesis Submitted to
the Graduate School of Engineering and Sciences of
İzmir Institute of Technology
in Partial Fulfillment of the Requirements for the Degree of

MASTER OF SCIENCE

in Molecular Biology and Genetics

by
Aslı ADAK

July 2017
İZMİR

We approve the thesis of **Aslı ADAK**

Examining Committee Members

_____
Assist. Prof. Dr. Gülistan MEŞE ÖZÇİVİCİ
Department of Molecular Biology and Genetics, Izmir Institute of Technology

_____
Assoc. Prof. Dr. Özden YALÇIN ÖZUYSAL
Department of Molecular Biology and Genetics, Izmir Institute of Technology

_____
Assist. Prof. Dr. Yavuz OKTAY
Izmir International Biomedicine and Genome Institute, Dokuz Eylül University

25 July 2017

_____
Assist. Prof. Dr. Gülistan MEŞE ÖZÇİVİCİ
Supervisor, Molecular Biology and Genetics,
Izmir Institute of Technology

_____
Prof. Dr. Volkan SEYRANTEPE
Head of Department of Molecular
and Genetics

_____
Prof. Dr. Aysun SOFUOĞLU
Dean of the Graduate School of
Biology Engineering and Sciences

ACKNOWLEDGEMENTS

I would like to express my deepest appreciation and thanks to my supervisor Assist. Prof. Dr. Gülistan MEŞE ÖZÇİVİCİ for her patience, encouragement, understanding, guidance and excellent support during my graduate studies.

Furthermore, I would like to thank to Assoc. Prof. Dr. Engin ÖZÇİVİCİ and Assoc. Prof. Dr. Özden YALÇIN ÖZUYSAL for their helps and guidance.

I am appreciated to family for their infinite support all over my life.

Also, I would like to thank The Scientific and Technological Research Council of Turkey – TUBITAK Grant 114Z874.

As last but not the least, I would like to thank to my lab mates who are Özgür ÖZTÜRK, Müge ANIL İNEVİ, Melis OLÇUM UZAN, Ece ŞAHİ, Begüm GÖKÇE, Müge BİLGEN, Öznur BASKAN and Şurhan GÖL for their supports and helps.

ABSTRACT

COMPARISON OF CONNEXIN32 EXPRESSION AND FUNCTION BETWEEN MCF10A NORMAL BREAST AND MDA-MB-231 BREAST CANCER CELL LINES

Breast cancer is one of the most prominent cancer-related deaths among females. Among many molecules, connexins have role in breast cancer. Gap junctions, formed from connexins (Cx), facilitate intercellular communication between adjacent cells. Different connexins were expressed during different stages of breast cancer. Cx32 was found both in normal pre-menopausal and tumor breast tissue samples. In lymph node metastases, elevated Cx32 level was observed compared to primary cancer. However, the role of Cx32 in breast cancer is not known but its elevation in lymph node metastasis may indicate its diverse functions in breast cancer.

To verify this, in MCF10A and MDA-MB-231 cell lines, Cx32 was overexpressed. The protein localization was compared with immunostaining. In MDA-MB-231 cells, Cx32 localized in nucleus and cytoplasm, although in MDA-MB-231 Cx32-EGFP cells, Cx32 localized mostly in the cytoplasm. In MCF10A cells, Cx32 localized in nucleus, whereas Cx32 formed gap junctional plaques between MCF10A Cx32-EGFP cells. By Cx32 overexpression, gap junction coupling increased in MCF10A cells significantly, although it did not change in MDA-MB-231 cells. In both cells, hemichannel activity was not altered with Cx32 overexpression. The effects of Cx32 overexpression on cell viability demonstrated a significant decrease in MCF10A cells and an increasing trend in MDA-MB-231 cells. Furthermore, the percentage of G_1 phase decreased, G_2 and S phases increased in MDA-MB-231. However, Cx32 overexpression did not alter cell cycle profile of MCF10A significantly. Determination of the differential role of Cx32 in different stages of breast cancer may help to understand its diagnostic and/or therapeutic potential.

ÖZET

CONNEXİN32'NİN İFADESİNİN VE FONKSİYONUNUN MCF10A NORMAL MEME HÜCRE HATTI VE MDA-MB-231 MEME KANSERİ HÜCRE HATTI ARASINDA KIYASLANMASI

Meme kanseri kadınlarda en çok ölüme sebep olan kanserlerden biridir. Diğer moleküllerin arasında, connexinlerin meme kanserinde rolü vardır. Gap junctionlar connexin proteinlerinden oluşup, yan yana olan hücrelerde hücreler arası iletişimi sağlamaktadır. Farklı connexin tipleri meme kanserinin farklı aşamalarında ifade edilmiştir. Cx32 hem normal menopoz öncesi meme dokusunda hem de tümör örneklerinde bulunmuştur. Cx32 ifadesinin lenf nodül metastazında, birincil meme kanserindeki ifadesinden daha fazla olduğu görülmüştür. Buna rağmen Cx32'nin meme kanserindeki rolü bilinmemektedir. Fakat Cx32 ifadesinin lenf nodül metastazında artması, Cx32'nin meme kanserinde, farklı fonksiyonlarının olduğunu gösterebilir.

Bunu doğrulamak için, Cx32 MCF10A'de ve MDA-MB-231'de fazla-ifade (*overexpression*) edildi. Proteinin yerleşimi floresan boyama ile karşılaştırıldı. MDA-MB-231 hücrelerinde Cx32 hücre çekirdeği ve sitoplazmasında yerleşirken, Cx32 fazla-ifade edilen MDA-MB-231 hücrelerinde çoğunlukla hücre sitoplazmasında yerleşmiştir. MCF10A hücrelerinde Cx32 hücre çekirdeğinde yerleşirken, fazla ifade edildiğinde yan yana olan hücreler arasında gap junctional plaka oluşturmuştur. Cx32 fazla-ifade edildiğinde, gap junction birlikteliğinin MCF10A hücrelerinde arttığı istatiksel olarak gözlemlenmiş olup, MDA-MB-231 hücrelerini etkilemediği görülmüştür. Cx32 fazla-ifadesi her iki hücre için de yarımkanal aktivitesini etkilememiştir. Cx32 fazla-ifadesi, MCF10A hücrelerinin çoğalmasını azalttığını ve MDA-MB-231 hücrelerinin çoğalmasına eğilim verdiğini göstermiştir. Ayrıca, G_1 fazının yüzdesinin azaldığını, G_2 ve S fazlarının yüzdesinin Cx32 fazla-ifade eden MDA-MB-231 hücrelerinde arttığını göstermiştir. Ancak Cx32 fazla-ifadesi MCF10A hücre döngüsü profilini değiştirmemiştir. Cx32'nin meme kanserinin gelişmesinin farklı aşamalarında fonksiyonlarının karar verilmesi, meme kanserinin tanı ve terapötik potansiyelini anlamamıza yardımcı olabilir.

TABLE OF CONTENTS

LIST OF THE FIGURES

Figure **Page**

LIST OF TABLES

CHAPTER 1

INTRODUCTION

1.1. Gap Junctions

Cells communicate among them in order to maintain homeostasis, therefore they sense and respond to the environmental conditions. One type of cellular communication is provided by gap junctions [1]. Gap junctions are intercellular channels found on the plasma membrane of adjacent cells at cell-cell contact sites (Figure1.1) [2]. By forming link between cells, gap junctions allow cells to coordinate their function [3]. Through gap junctions, ions (K^+ and Ca^{2+}), small metabolites (glucose) and second messengers (cGMP, cAMP, and inositol 1,4,5-triphosphate (IP_3)) can pass and thereby enable electrical and biochemical communication between cells [1]. Thousands of gap junctions can form plaques by clustering on the membrane (Figure 1.1). The close proximity of adjacent membranes is essential to form docking by leaving a 2-nm gap [4].

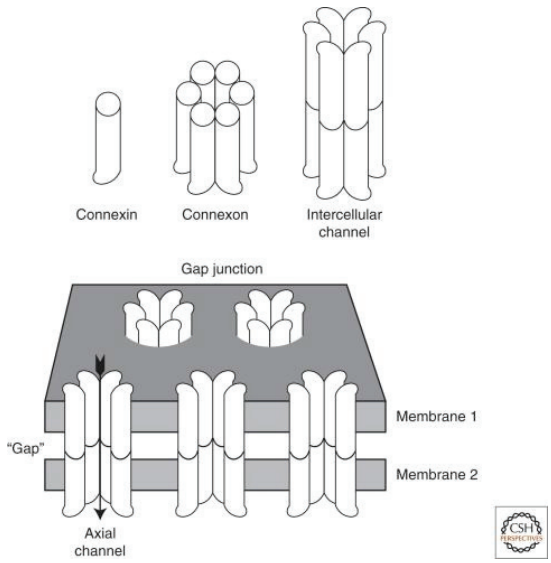

Figure 1. 1. Formation of gap junctions and gap junction plaques: Six connexin proteins form connexon which docks with another connexon from an adjacent cell and form gap junction. Gap junctions cluster on the membrane and construct plaques [4].

1.2. Hemichannels

Gap junctions are formed by two connexons or hemichannels, each of which is provided by one of the contacting cells. Hemichannels are built by six connexin (Cx) proteins (Figure 1.1) [5]. Through these hemichannels, signaling molecules, e.g. PGE_2, ATP and NAD^+, can be excreted that can mediate intracellular signaling response by affecting the cells with paracrine or autocrine signaling [6].

Hemichannels were shown to play role in calcium signaling and cell proliferation in addition to the normal functions and development of the cells [7]. Further, as gap junctions do, hemichannels also play role in cell survival and death [5]. For example, hemichannels built by Cx43 were found to act on the survival signal transduction by mimicking of the ERK-activating/anti-apoptotic impact of bisphosphonates [8].

Hemichannels can shift from open to closed conformation and vice versa by different stimuli. The probability of hemichannel opening increases with low $[Ca^{2+}]$, positive membrane potentials ($+V_m$), pharmacological agents e.g. quinine and quinidine, dephosphorylation and reactive oxygen species (ROS). However, the probability of hemichannels closing increases with high $[Ca^{2+}]$, negative membrane potentials ($-V_m$), polyvalent cations e.g. Co^{2+}, Ni^{2+}, Mg^{2+}, La^{2+} and Gd^{3+} and low intracellular pH (Figure 1.2). Mechanisms controlling hemichannels and their openings, affect the exchange of ions and small molecules between the cytoplasm and the extracellular space [9].

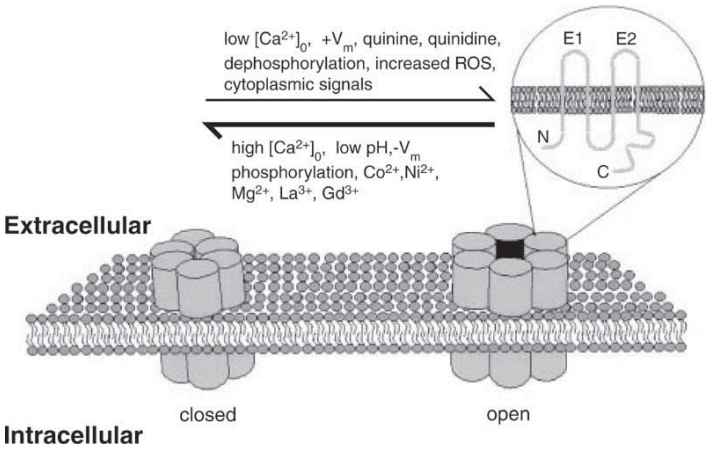

Figure 1. 2. Conditions opening and closure of hemichannels. Conditions leading to opening of hemichannels are indicated with right side arrow while conditions leading to closure of hemichannels are indicated with left side arrow [9].

1.3. Connexins and Their Structure

Both vertebrates and invertebrates have gap junctions. In nonchordate animals, gap junctional channels are encoded by innexin (Inxs) gene family [10], while in chordate animals, they are encoded by connexin gene family [11]. Although the gap junctions formed by innexins or connexins have similarities in function, innexins and connexins are not homologous [1]. In vertebrates, recently another protein group, called pannexins (Panxs) were identified. Pannexins are believed to be related to innexins distantly and they were found to be expressed in kidney, eye, and neuron tissues [12].

In almost every mammalian cells, gap junctional intercellular communication (GIJC) is found, indicating the importance of gap junctions in tissue homeostasis. Family of connexins has 21 members in humans and 20 members in mouse. Although the channels formed by connexins have common roles in tissues, the differential functions of channels are considered as a result of expressed connexin type in single cells [13].

Connexins (Cxs) are transmembrane proteins that traverse the membrane four times and form hexameric complexes (hemichannels) in the membrane. Two extracellular (EC) loops (EC1, EC2) and a cytoplasmic loop (CL) join four transmembrane (TM) helices (TM1-TM4) in a connexin protein (Figure 1.3) [14].

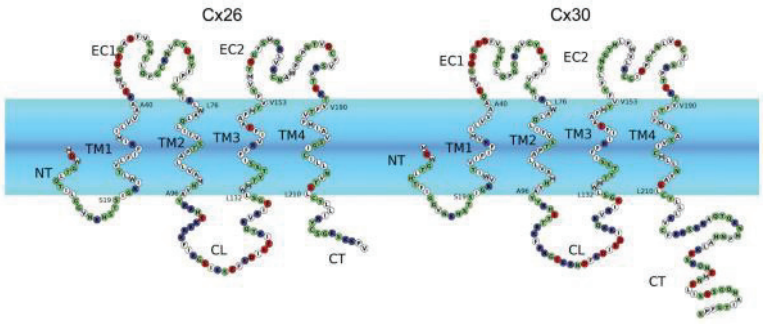

Figure 1. 3. Representation of hCx26 and hCx30 topology. NT stands for N-terminus; CT C-terminus; TM, transmembrane helices; CL, cytoplasmic loop; EC, extracellular loop. Color representation code: blue, positive; red, negative; white, hydrophobic and green, hydrophilic [14]

Connexins are named in two different ways: the first way uses the origin of connexin species and their molecular mass in kDa. As an example, mCx32 represents mouse connexin 32 protein which is about 32 kDa. Secondly, connexins can be sub-

grouped into α, β, γ, δ or ε according to sequence identity and cytoplasmic loop length. Abbreviation as "Gj" for "Gap junction" and numbering according to its discovery order is the way of connexins' representation. As an example, mCx43 can also be named as Gjα1 which means it is the first discovered connexin among α-group members [15].

Connexins can form hemichannels by contribution of the same type or different types which results in homomeric or heteromeric hemichannels, respectively. The upper level of complexity is seen during the formation of functional gap junctional channels. If the same homomeric hemichannels or the same heteromeric hemichannels form the channel, this gap junction is called homotypic. On the other hand, if different homomeric hemichannels or different heteromeric hemichannels form the channel, this gap junction is called heterotypic (Figure 4). Which type of hemichannels and gap junctions can be formed depends on the connexin types forming the channels, because compatibility among connexins is important during channel formation. For example, Cx26 can form heteromeric channels with Cx32, although it is not possible for Cx26 to form functional channels with Cx40 [1].

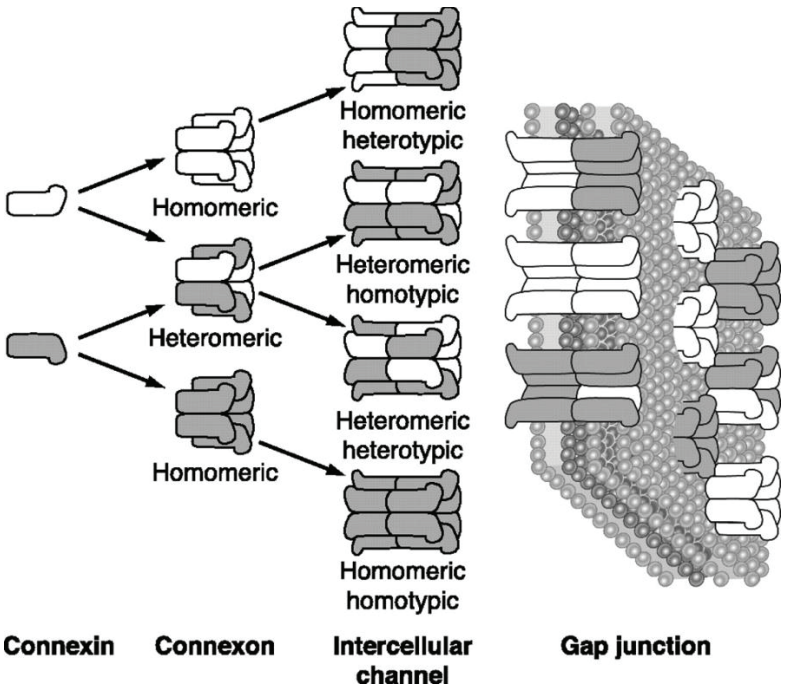

Figure 1. 4. Formation of different type of intercellular channels [16].

In humans, it would be thought that 21 types of gap junctional channel are possible if only homomeric hemichannels would occur and these hemichannels connect to the same types. Nevertheless, once the compatible connexins are expressed in the same cell, the chance of having different types of hemichannels and gap junctions increases. For example, in liver heteromeric Cx26/Cx32 [17], in the lens Cx46/Cx50 [18-19] and in the cochlea Cx26/Cx30 hemichannels [20] were shown to form. If a cell expresses 2 types of connexins, 14 possible hemichannels can form and with those hemichannels 196 type of gap junctions can form. However, the complexity is much more since some cell types can express more than two types of connexins. For example, epidermis has shown to express more than seven different connexins during keratinocyte differentiation. Nevertheless, this diversity is limited with the fact that only compatible connexins can form hemichannels [13]. This complexity is important because heteromeric/heterotypic channels have diverse properties than their homomeric/homotypic counterparts e.g. gating, conductance and permeability and therefore influence cell function differently [21].

1.4. Gap Junction Selectivity

Ions and small molecules having less than 1kDa molecular mass can pass through gap junctions. Beside molecular weight and size of the molecules, their net charge, shape and interactions with connexins play role in determining their ability to pass through gap junctions [22]. Intracellular messengers e.g. cAMP, cGMP, IP_3 and tracers e.g. Neurobiotin, Biocytin can pass through gap junctions. The conduction of a gap junction depends on the connexin types forming the junctions. With the site-specific mutation studies, the conductance, selectivity of ions and permeability were shown to depend on the N-terminal domain amino acid sequence. Other two factors determining the conductivity are the number of channels forming the plaque and status of opening and the ratio of open pores at that time [23].

1.5. Connexin Biosynthesis

Connexins are produced in ribosomes bound to Endoplasmic Reticulum (ER) and they are inserted into the ER membrane co-translationally (Figure 1.5) [24]. As an

exception of this pathway, Cx26 can be both inserted post- and co-translationally to the ER membrane [25]. Oligomerization of the connexins into hemichannels can happen either in the ER–Golgi intermediate compartment (ERGIC) or trans Golgi network (TGN) (Figure 1.5), depending on the type of connexin [24]. For example, Cx32 oligomerization occurs in ERGIC [24], although Cx43 and Cx46 oligomerization occurs in TGN [13, 26]. Correctly folded connexin proteins exit the ER and enter into *cis*-Golgi network [13]. However, Cx26, as an exception, can directly get to the cell membrane with Golgi-independent pathway [27]. After oligomerization, connexons are transported to the plasma membrane (PM) with the vesicles carried on microtubules. Then, the vesicles fuse with the non-junctional PM. After this transport, connexons can reach to gap junctional plaque region by moving laterally on the PM (Figure 1.5) [28].

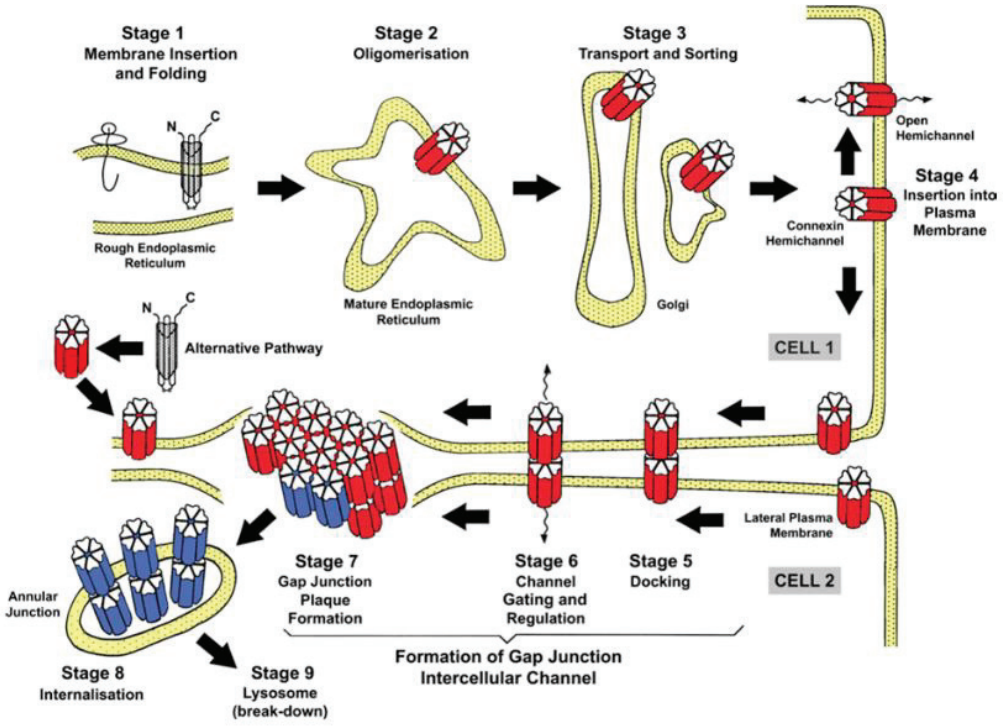

Figure 1. 5. Assembly and break down of gap junctions. Hemichannels form in the early stage of secretory pathway (stage 1) and those hemichannels carried with the secretory pathway (stages 2 and 3). Another assembly mechanism is seen for Cx26 that is direct assembly into membrane with Golgi independent pathway. After insertion into the membrane (stage 4), hemichannels dock with its partner from the adjacent cell (stage 5) and form functional gap junctions (stage 6). If the gap junctions aggregate, they form plaques in the membrane (stage 7). During stage 7 and stage 8, gap junctions can be internalized and they are broken down in lysosome (stage 9) [29].

1.6. Regulation of Gap Junction Channels Gating

Gating is a term used for defining adjustment in opening and closing of the channels. This also can mean that channel is available or unavailable to conduct. The activity of gap junctions is regulated by voltage, calcium concentration change and phosphorylation [30].

Transjunctional voltage: In excitable cells, sensitivity of voltage plays role in intercellular coupling regulation [31]. Hemichannels forming gap junction contains two transjunctional voltage (Vj) sensitive gates [32]. The fast gate is found in the hemichannels of cytoplasmic entrance side. This fast gate modulates the open to residual state. However, the slow or loop gate is found on the extracellular side of hemichannels and it mediates closing state transitionally [31] .

Intracellular Ca^{2+}: Intracellular Ca^{2+} leads to the closure of the channels, which is very important for the cells to prevent from depolarization of the membrane and metabolite leakage from the gap junctions by separating them [31].

Intracellular pH: The sensitivity of the connexins to the intracellular pH varies according to the type of connexin [31]. For example, Cx38 and Cx57 are more sensitive to pH than Cx32 and Cx43 [33-34]. Permeability of gap junction channel changes with the protonation of the histidine residues in cytoplasmic loop and carboxyl tail [31]. It was seen that increase in intracellular pH increased the probability of channel opening and functional channel numbers [34]. However, for Cx36 GJ channels, the pH was shown to has the opposite effect, which means when pH increases, the activity of channels decrease [35].

Phosphorylation: There are multiple serine, threonine and tyrosine residues on the cytoplasmic C-tail of the connexins and these residues can be phosphorylated by different protein kinases [31]. However, Cx36 phosphorylation can be performed on the cytoplasmic loop as well [36]. Since the molecular structure of connexins and their interacting partners can change with phosphorylation status, it affects the electrical and metabolic interaction of the adjacent cells, integrity of channels, mean open time or the probability of opening the channel [31]. For example, in *Xenopus* oocytes, the opening of hemichannels formed by Cx46 was reduced with protein kinase C (PKC) activation [37].

1.7. Connexins in Human Physiology

Since the features of gap junctions formed by different connexins are diverse, loss of one form cannot be compensated with another one. Therefore, even a single connexin gene is mutated, the types of channels can be affected and can result in different types of diseases [21]. As it is shown in Table 1.1, ten different connexin gene mutations have been associated with twenty-eight genetic diseases. For example, mutation on the Cx32 gene leads to Charcot- Marie- Tooth disease which is a heritable peripheral nerve disease [38]. Cx46 and Cx50 mutations cause cataract which results in the clouding of the lens [39]. Mutations on the Cx26, Cx30, Cx30.3 and Cx31 genes lead to deafness and skin disorders [40].

Table 1. 1. Genetic disorders associated with human connexin mutations [21]

Gene	Chromosome	Protein	Disorder(s)
GJA1	6q22.31	Cx43	Craniometaphyseal dysplasia, autosomal recessive Erythrokeratodermia variabilis et progressiva Oculodentodigital dysplasia Syndactyly, type III
GJA3	13q12.11	Cx46	Cataract
GJA5	1q21.2	Cx40	Atrial fibrillation, familial, 11 Atrial standstill, digenic (GJA5/SCN5A)
GJA8	1q21.2	Cx50	Cataract
GJB1	Xq13.1	Cx32	Charcot-Marie-Tooth neuropathy, X-linked 1
GJB2	13q12.11	Cx26	Bart-Pumphrey syndrome Deafness, autosomal dominant 3A Deafness, autosomal recessive 1A Porokeratotic eccrine ostial and dermal duct nevus
GJB3	1p34.3	Cx31	Deafness, autosomal dominant 2B Deafness, digenic, (GJB2/GJB3) Erythrokeratodermia variabilis et progressiva
GJB4	1p34.3	Cx30.3	Erythrokeratodermia variabilis et progressiva
GJB6	13q12.11	Cx30	Deafness, autosomal dominant 3B Deafness, autosomal recessive 1B
GJC2	1q42.13	Cx47	Leukodystrophy, hypomyelinating, 2 Spastic paraplegia 44, autosomal recessive Lymphedema, hereditary

In addition to genetic diseases, direct intercellular communication was hypothesized to be related with the cancer onset and progression, since tumor cells were observed to lack electrical coupling. Following studies combined this hypothesis with the connexins [41]. Connexins and GJs were considered in tumor suppression [42]. However, it was observed in the later studies that connexins are regulated in context dependent manner [43].

1.8. Connexin Expression in Human Mammary and Developing Mammary Gland

During development and differentiation of mammary gland, it needs intercellular communication, which can be supplied through gap junctions. Further, during development and differentiation of mammary gland the functions of channels and expression of the connexins are regulated dynamically [44].

In the mammary gland of human, Connexin 26 (Cx26) message was first found in epithelial cells [45]. In later studies, other connexins were also detected in normal mammary epithelial cells. In 1992, Cx43 was found firstly in the in mammary gland [46]. With further experiments to understand the localization of Cx43, it was shown that Cx43 was detected in myoepithelial cells [47]. In addition to this, Cx43 was shown to localize between luminal cells of gland ducts [48]. Cx26 was shown mostly to localize in the ducts myoepithelium in human gland and less in lobular/alveolar structures [49], (Figure 1.6).

Since obtaining samples from human breast tissue during all of the differentiation stages is difficult, mouse samples have been used to study on the role of connexins during the mammary gland development [44]. Cx26 was detected in mouse mammary gland during lactation [47] and then, it was found during all stages of development involving virginity to involution, peaking during lactation period [50-52]. On the other hand, Cx30 mRNA expression was found in mammary gland of pregnant and lactating mouse [50, 53]. Cx30 protein expression was shown at pregnancy day 15 and its expression reaching a peak at lactation and then decreasing in involution [53].

Cx32 mRNA expression was found at parturition and lactation periods [47, 51]. Although in some studies Cx32 protein expression was concluded to be expressed only in lactating gland [51, 54], in another study Cx32 expression was detected at all stages of development gland in situ [53]. In this study, Cx32 was found to be expressed at low

levels in virgin and involuting gland, whereas expressed at high levels in the lactating gland [53].

Cx43 mRNA was found to be downregulated during mid-pregnancy and almost not expressed during lactation and start to be expressed after involution again [53, 55]. As it is shown in Figure 1.6, Cx43 proteins are localized between the basal myoepithelial cells [47].

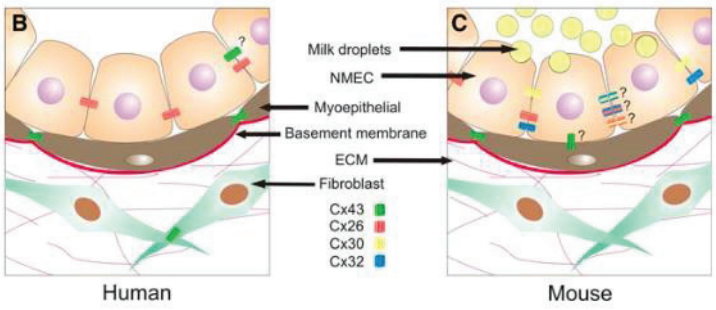

Figure 1. 6. Connexin expression in human and mouse mammary gland. B. In human breast tissue, Cx43 (represented with green color) channels are found between myoepithelial cells although Cx26 (represented with red color) channels are in between luminal cells. In addition to this Cx43 can be found in human fibroblast cells in stroma. C. Similar to human mammary gland, in mouse mammary gland Cx43 channels are found between myoepithelial cells and Cx26 channels are localized between luminal cells. In addition to this, Cx30 (represented with yellow color), and Cx32 (represented with blue color) are expressed in luminal cells and they reach to the peak during lactation [44].

1.9. Breast Cancer and Connexins

Breast cancer constitute 23% of all cancer cases and it is one of the most prominent cancer deaths among females [56]. Among many molecules, connexins and gap junctional communication were shown to have role in breast cancer [57]. Cx26 and Cx43 were shown to be downregulated at the level of mRNA in human breast primary tumors [58] and breast cancer cell lines [48].

In contrast to tumor suppressor role of connexins, upregulation of connexins in breast cancer tissues has also been reported in several studies [44]. Cx43 was firstly found in benign and normal tissue as well as myoepithelial cells of ductal carcinoma in situ (DCIS) [59].

Human mammary carcinoma cells MDA-MB-435 was transfected and stable cells were generated with hCx26 or hCx43. In both cells, the growth rate and tumor forming capability of the cells were decreased [60]. Overexpression of Cx43 or Cx26 lead to tumor-suppressive effect on MDA-MB-231 in three-dimensional organoids by reducing anchorage-independent growth [61]. Overexpression of Cx26 and Cx43 in MDA-MB-231 cells reduced cell migration and led to change from mesenchymal to epithelial phenotype. Also, this overexpression was observed to regulate angiogenesis by reducing it [62]. Beside overexpression of connexins, when Cx43 was silenced in Hs578T cells, it led to an increase in cell growth and migration capacity [63]. In contrast to this, the involvement of connexins in invasion and metastasis is considered more complex, depending on cell type and tumor stages [57].

Cx26 and Cx43 were implicated in human breast where they are downregulated and so do not form GJs. There are other studies showing an increase in connexin expression in later stages [57]. In one of these studies, expression of Cx26 and Cx43 in primary tumor and lymph node metastasis were compared. Cx26 protein expression detected in 53 % of primary tumors and Cx43 protein expression was detected in 82 % of primary tumors. In lymph node metastasis cases, these proportions increased to 88 % for Cx26, 96 % for Cx43 proteins [64]. In another study, MDA-MB-231 cell line and its bone metastatic variant, B02, were compared in terms of their gene expression. It was seen that Cx43 mRNA was expressed five-fold higher in the B02 cells, which was also confirmed with quantification of protein levels [65]. Therefore, as cancer advances, connexins can be upregulated transiently in the later stages of metastasis, which was proposed to be the case for the breast cancer as well, as it is shown in Figure 1.7 [57].

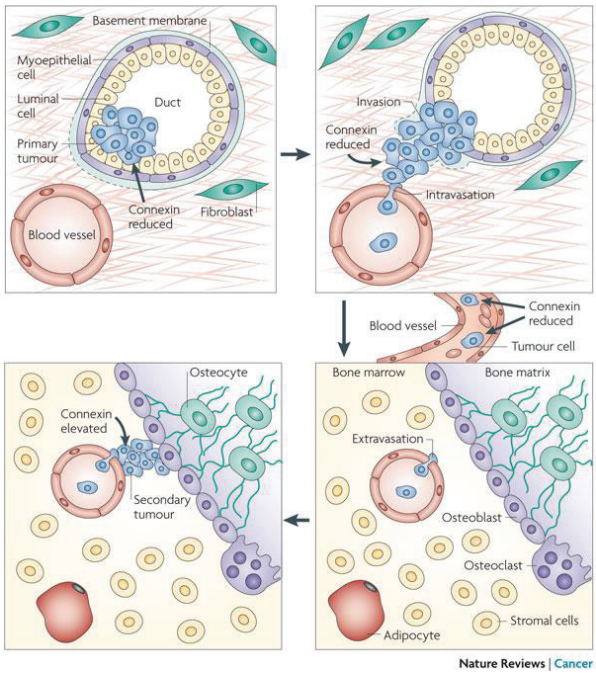

Figure 1. 7. Proposed connexin regulation during breast cancer stages. Onsets of breast cancer: invasion, intravasation, extravasation and metastasis are illustrated [57].

Cx32 was shown to play role in hepatocellular carcinomas (HCCs). For example, GJIC mediated by Cx32 was found to suppress the HCCs development but cytoplasmic Cx32 protein had positive effect on HCC progression [66]. It was also shown that increase in Cx32 suppressed HCC invasion and migration as well as its cell proliferation [67]. Further, it was demonstrated that invasion and metastasis of HCC were inhibited by Cx32 through Snail-mediated epithelial-mesenchymal transition [68]. In another study, Cx32 expression was found to decreased as HCC progressed and the localization of the protein changed. It became internalized in HCCs [69]. These suggested that cytoplasmic and plasma membrane bound Cx32 may have different roles in HCC fate. In addition to Cx32 in HCC, Cx32 expression was also found both in normal pre-menopausal breast tissue and tumor samples taken from patient [70]. In another study, elevated levels of Cx32 was seen compared to primary breast cancer in lymph node metastases [71]. Taken all of these together Cx32 might be important factor for cancer. However, the role of Cx32 in breast cancer is not exactly known. Based on these, it was hypothesized that Cx32 may have different roles in breast cancer initiation and/or progression.

1.10. Aim of the Project

The aim of the project was to investigate the role of Cx32 in breast cancer by comparing its impacts on MDA-MB-231 and MCF10A cells. Therefore; Cx32 was overexpressed in MDA-MB-231 invasive breast cancer and MCF10A normal breast cells and the effect of the Cx32 overexpression was assessed in terms of cell proliferation and regulation of cell cycle.

CHAPTER 2

MATERIALS AND METHODS

2.1. Maintenance of MDA-MB-231 and MCF10A

MDA-MB-231 cells were grown in high glucose Dulbecco's Modified Eagle Medium (DMEM) (GIBCO, Cat# 11965092) which was supplemented with 10 % Fetal Bovine Serum (FBS) (GIBCO, Cat# 16000044) and Penicillin-Streptomycin (GIBCO, Cat # 15140122). MDA-MB-231 cells were split twice a week with 0.05 % Trypsin-EDTA (Biological Industries, Cat# 03-053-1A) incubation for 5 min at 37 °C.

MCF10A cells were grown in DMEM/F-12 medium which was supplemented with 5% Donor Horse Serum (Biological Industries, Cat# 04-004-1B), 1% Penicillin/Streptomycin (GIBCO, Cat # 15140122), 20ng/mL EGF (Sigma, Cat# E9644), 0.5 µg/mL Hydrocortisone (Sigma, Cat# H0888), 100ng/mL Cholera Toxin (Sigma, Cat# C8052-0.5MG) and 10 µg/mL Insulin (Sigma, Cat# I1882-100MG). MCF10A cells were split twice a week with Trypsin-EDTA (Biological Industries, Cat# 03-053-1A) incubation for 15 min at 37°C. Both cells were cultured in an incubator with 37 °C temperature and 5% CO_2.

2.2. Transfection

After plating $4x10^5$ MDA-MB-231 cells/well in a 6-well plate, cells were incubated for 48 hours. Cells were transfected with 2µg/6µl DNA/Fugene HD ratio containing Opti-MEM® (Thermo Fisher, Cat# 31985062) by following manufacturer's protocol.

After plating $5x10^5$ MCF10A cells/well in 6-well plate, cells were incubated for 24 hours. Cells were transfected with 2µg/4µl DNA/Fugene HD ratio containing Opti-MEM® (Thermo Fisher, Cat# 31985062) by following manufacturer's protocol.

2.3. Virus Production

24 hours after plating 3.5-4.5x10^6 293T cells in 10cm plates, cells were transfected with the lentiviral plasmids: 2µg pLenti-GIII-CMV-GFP-2A-Puro (pLenti-GFP) or 2µg pLenti-GIII-CMV-GFP-2A-Puro-Cx32 (pLenti-Cx32-GFP) together with 1.3µg packaging vector (pCMVdR8.74) and 0.7µg envelope vector (pMD2.VSVG) using 12 µl Fugene HD. 24 hours after transfection, the medium of the cells was aspirated and 8.5 mL fresh medium was added on cells. 48 hours after transfection, the medium containing viruses was collected into falcon tubes and fresh 8.5 mL medium was added on cells. The collected virus was kept at 4°C until the next collection. After 72 hours of infection, the virus containing medium was collected. For titration, 200 µl of virus was aliquoted and they were all stored at – 80°C.

2.4. Virus Titration

In order to determine the efficiency of the virus production, virus titer was determined. Virus titration was done by using mouse fibroblast NIH3T3+ cells. After 24 hours of plating 2x10^5 NIH3T3+ cells to 6-well plate, the diluted viruses (with 10^{-3}, 10^{-4}, 10^{-5} concentrations) with 4mL final volume containing 8 µg/mL polybrene was added on cells in each well. The plates were centrifuged for 2 hours with 2,500 rpm at 32°C. Then, 2 mL fresh medium was added on cells. 48 hours after infection, the cells were trypsinized and transferred to 10 cm plate with the addition of selection medium containing 2 µg/mL puromycin. The selection was maintained until all the cells in mock condition were dead.

2.5. Crystal Violet Staining

Once the selection was completed, the plates were washed with 1X PBS twice under the hood. After the addition of 4 mL 1X PBS, the plates were transferred to the bench and the PBS was aspirated. The plates were then incubated with 5 mL of 0.5 % Crystal Violet staining solution for 10 min on a shaker at room temperature. Then, the Crystal Violet staining solution was removed and the plate was rinsed with 1X PBS. 10 min washing with 1X PBS was repeated until the mock plate becomes transparent. After

removing 1X PBS, the plates were inverted and left to dry. The colonies on dried plates were counted.

2.6. Infection

$3.5x10^5$ MDA-MB-231 cells/well and $2.5x10^5$ MCF10A cells/well were plated on 6-well plates. After 24 hours, the medium of the cells was aspirated and 4 mL of virus containing 8 μg/mL polybrene was added on cells in each well. The plates were centrifuged for 2 hours with 2,500 rpm at 32°C. Then, 2 mL fresh medium was added on cells. 48 hours after infection, the cells were trypsinized and transferred to 10 cm plate with the addition of selection medium containing 2 μg/mL puromycin. The selection was maintained until all the cells in mock condition were dead.

2.7. Immunostaining and Fluorescence Imaging

MDA-MB-231 and MCF10A cells were plated on coverslips in 6-well plates. The method was performed 24 hours after plating for MCF10A or 48 hours for MDA-MB-231 cells. After rinsing the cells twice with 1X PBS, the cells were fixed by using 4% PFA in 1X PBS for 20 min at room temperature. Then, the cells were rinsed with 1X PBS three times and permeabilized with 0.1 % TritonX-100/PBS for 15 min at room temperature. Cells were blocked with 3 % BSA (Amresco, Cat# 0332-1006) in 0.1 % TritonX-100/PBS for 30 min at room temperature. After the cells were incubated with 1:200 dilution of polyclonal rabbit anti-Cx32 antibody for 1 hour at room temperature, cells were washed three times with 1X PBS for 10 min each. Then the cells were incubated with 1:200 dilution of Alexa488-conjugated goat anti-rabbit secondary antibody and 1:1000 dilution of DAPI for 1 hour at room temperature in the dark. After the cells were washed three times with 1X PBS, the coverslips were dipped into autoclaved water, dried and mounted on a slide. The images of the samples were taken with Olympus CKX71 fluorescent microscope and images were analyzed with Image J program.

2.8. qRT-PCR Analysis

48 hours after transfection of MDA-MB-231 cells and 24 hours after transfection of MCF10A cells, the cells were rinsed twice with 1X PBS and they were flash-frozen. For stable cells (both of MDA-MB-231 and MCF10A cells), 48 hours after plating, the cells were rinsed twice with 1X PBS and they were flash-frozen.

The total RNA was isolated from MCF10A and MDA-MB-231 cells by using PureLink® RNA Mini Kit (Liftech, Cat# 12183018A) according to manufacturer's protocol. The isolated RNA concentration and purity was measured with Nano drop. 1 µg cDNA was synthesized by using cDNA Synthesis Kit (ThermoFisher, Cat# K1622) according to manufacturer's protocol. cDNAs were used for the genes listed in Table 2.1 by using their respective primers with the protocol indicated in Table 2.2.

Table 2. 1. Genes and respective primers used for qRT-PCR

Gene	Forward Primer	Reverse Primer
Human Cx32	5'-ggcacaaggtccacatctca-3'	5'-gcatagccagggtagagcag-3'
EGFP	5'-acgtaaacggccacaagttc-3'	5'-aagtcgtgctgcttcatgtg-3'
Human GAPDH	5'-gaaggtgaaggtcggagtca-3'	5'-aatgaaggggtcattgatgg-3'

Table 2. 2. Protocol for qRT-PCR

Preincubation	95 °C	600 s	1 cycle
3 step amplification	95 °C	30 s	45 cycle
	60 °C		
	72 °C		
Melting	95 °C	10 s	1 cycle
	65 °C	60 s	
	72 °C	1 s	

2.9. Scrape Loading

After 48 hours of plating MDA-MB-231 cells, they were rinsed with 1X PBS. Then, 0.5 mg/mL Neurobiotin (NB) tracer (Vector Laboratories, Cat# SP-1120) containing Opti-MEM® (Thermo Fisher, Cat# 31985062) were added on cells. After making cuts with scalpel blade, cells were incubated for 10 min at 37°C. Then, the NB containing Opti-MEM® was aspirated, DMEM medium was added and cells were incubated for 20 min at 37 °C. After washing with Opti-MEM® three times (10 min each) at 37 °C, cells were fixed with 4 % Paraformaldehyde (PFA) for 15 min at room temperature. The cells were rinsed with 1X PBS three times and they were permeabilized with 0.1 % TritonX-100/PBS for 15 min at room temperature. Then, cells were blocked with 3 % BSA (Amresco, Cat#0332-1006) overnight at 4 °C. After cells were incubated with Rhodamine-conjugated streptavidin (ThermoFisher, Cat# 21724) with 1:500 dilution and DAPI with 1:1000 dilution in blocking solution for 1 hour at room temperature, they were washed with 1X PBS for 10 min twice. Then, 1X PBS was added and the samples were kept in 4 °C until imaged.

After 48 hours of plating MCF10A cells, they were rinsed with 1X PBS. Then, 0.5 mg/mL Neurobiotin (NB) tracer (Vector Laboratories, Cat# SP-1120) containing 1X PBS were added on cells. After making cuts with scalpel blade, cells were incubated for 10 min at 37°C. Then, the NB containing 1X PBS was aspirated, cells were incubated in fresh DMEM/F-12 medium for 20 min at 37°C. After washing with 1X PBS three times (10 min each) at 37°C, cells were fixed with 4 % Paraformaldehyde (PFA) for 15 min at room temperature. The cells were rinsed with 1X PBS three times and they were permeabilized with 0.1 % TritonX-100/PBS for 15 min at room temperature. Then, cells were blocked with 3 % BSA (Amresco, Cat#0332-1006) overnight at 4 °C. After cells were incubated with Rhodamine-conjugated streptavidin (ThermoFisher, Cat# 21724) with 1:500 dilution and DAPI with 1:1000 dilution in blocking solution for 1 hour at room temperature, they were washed with 1X PBS for 10 min twice. Then, 1X PBS was added and the samples were kept in 4 °C until imaged.

2.10. Dye Uptake

After 48 hours of plating MDA-MB-231 cells, they were rinsed with 1X PBS. Then, cells were incubated with Opti-MEM® for 20 min at 37 °C. After, cells were incubated with 0.5 mg/mL Neurobiotin (NB) tracer (Vector Laboratories, Cat# SP-1120) containing Opti-MEM® for 20 min at 37 °C, cells were washed with DMEM medium three times (10 min each) at 37 °C. After fixation, the experiment was completed as explained in Section 2.9.

After 48 hours of plating MCF10A cells, they were rinsed with 1X PBS. Then, cells were incubated with 1X PBS for 20 min at 37°C. After, cells were incubated with 0.5 mg/mL Neurobiotin (NB) tracer (Vector Laboratories, Cat# SP-1120) containing 1X PBS for 20 min at 37 °C, cells were washed with 1X PBS three times (10 min each) at 37 °C. After fixation, the experiment was completed as explained in Section 2.9.

2.11. MTT Assay for Cell Viability

$2x10^3$ MCF10A and MDA-MB-231 cells/well were plated in 48-well plate. On day 1, 4, 7 and 10, cells were incubated with medium containing 10% 3-(4,5-Dimethylthiazol-2-yl)-2,5-diphenyltetrazolium bromide (MTT) solution for 4 hours at 37°C with 5% CO_2. After removing medium containing MTT solution from cells, the crystals were solubilized by adding DMSO and the solution was transferred to 96-well plate for measurement. The absorbance of the samples was measured with spectrophotometer at 570 nm and 650 nm.

2.12. PI Staining for Cell Cycle Analysis

$4x10^5$ MCF10A and MDA-MB-231cells/well were plated in 6-well plate. After 48 hours, the cells were rinsed with 1X PBS. After trypsinization, the cells were collected in falcon tubes and centrifuged for 10 min at 1,200 rpm. The supernatant was aspirated and the pellets were put on ice. After addition of 1 mL cold 1X PBS, cells were pipetted gently. After addition of 4 mL cold 100 % EtOH, the suspension was mixed gently. The falcons were incubated at –20 °C at least overnight. Following centrifuging at 1,500 rpm for 10 min, they were centrifuged at 2,000 rpm for 1 min. The

supernatant was aspirated and 1mL PBS added. After the solutions were transferred to the Eppendorf tubes, they were centrifuged at 1,500 rpm for 10 min at +4°C. The supernatant was aspirated, 200 µl 0.1 % TritonX-100/PBS and 20 µl RNase A (200 µg/mL) were added, mixed well and incubated at 37°C for 30 min. After the solutions were transferred to flow cytometer tubes, 20 µl PI (1mg/mL) was added and incubated at dark for 15 min. The analysis of cell cycle was performed with FACS Canto (BD Biosciences, CA, USA).

CHAPTER 3

RESULTS

3.1. Localization of Cx32 in MDA-MB-231 and MCF10A cells

The overexpression of Cx32 can change the localization of the protein and for this reason the localization of the Cx32 was controlled. Untransfected, pIRES2-Cx32-EGFP2 and pIRES-EGFP transfected MDA-MB-231 and MCF10A cells were stained with immunohistochemistry method using anti-Cx32 antibody and Alexa555-conjugated goat anti rabbit secondary antibody. In addition to this, DAPI was used to visualize the nuclei of cells (Figure 3.1).

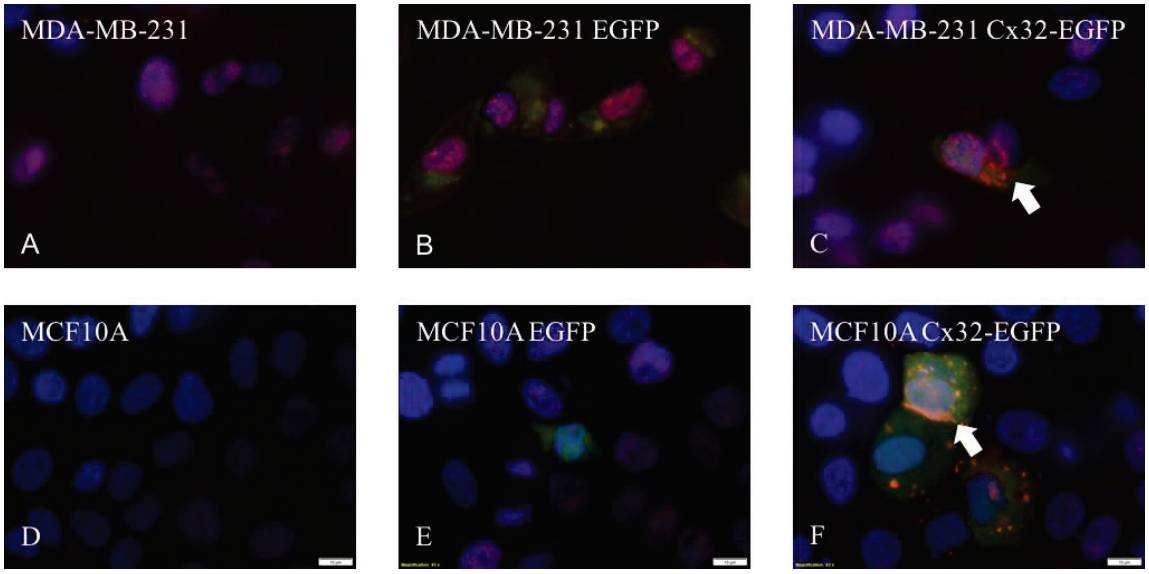

Figure 3. 1. Immunostaining of MDA-MB-231 and MCF10A cells with Cx32. Images were taken with fluorescence microscope at 100X magnification (scale bar: 10 μm) A) Untransfected MDA-MB-231cells B) pIRES2-EGFP2 transfected MDA-MB-231 cells C) pIRES2-Cx32-EGFP2 transfected MDA-MB-231 cells D) Untransfected MCF10A cells E) pIRES2-EGFP2 transfected MCF10A cells F) pIRES2-Cx32-EGFP2 transfected MCF10A cells. Red color represents Cx32, green color represents GFP and blue color represents nucleus of the cells.

In Figure 3.1 A it is observed that Cx32 was localized in nucleus and cytoplasm in untransfected MDA-MB-231 cells; whereas Cx32 was mostly localized in nucleus in untransfected MCF10A cells (Figure 3.1 D). It is observed in Figure 3.1 C that in MDA-MB-231 Cx32-EGFP cells, white arrow shows Cx32 proteins were localized more in the cytoplasm. In Figure 3.2 F, white arrow shows that Cx32 proteins formed gap junctional plaques between the adjacent cells when Cx32 was overexpressed.

3.2. mRNA Levels of Cx32 in MDA-MB-231 and MCF10A Transient Cells

mRNA levels of MDA-MB-231 and MCF10A cells were controlled with qRT-PCR and they were normalized to GAPDH housekeeping gene individually. After this, the Cx32 mRNA levels were normalized to untransfected mRNA levels of respective cell type. The mRNA levels for Cx32 increased approximately $5x10^5$-fold for MDA-MB-231 and approximately $5x10^4$-fold for MCF10A compared to untransfected cells as a result of transfection (Figure 3.2). Although the increase in MDA-MB-231 cells was statically significant ($p< 0.01$ ***, n=2), it was not significant for MCF10A cells.

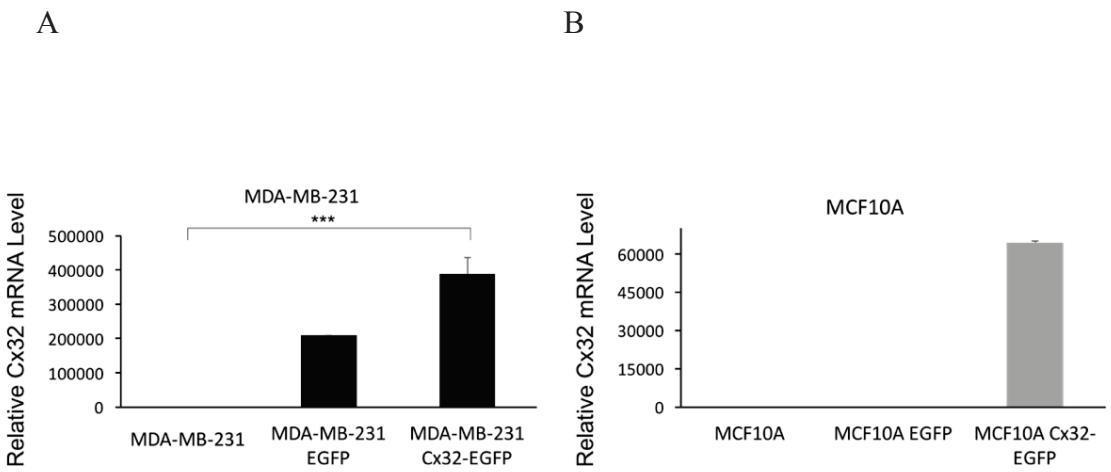

Figure 3. 2. Relative Cx32 mRNA levels of MDA-MB-231 (A) and MCF10A (B) cells transfected with pIRES-EGFP or pIRES-Cx32-EGFP vectors. They were normalized to Cx32 mRNA levels of untransfected MDA-MB-231 and MCF10A, respectively ($p< 0.01$ ***, n=2).

3.3. mRNA Levels of Cx32 in MDA-MB-231 and MCF10A Stable Cells

MDA-MB-231 and MCF10A cells were infected with both pLenti-GFP and pLenti-Cx32-GFP vectors and stable cell lines were obtained after the selection. After the cells in mock condition died, the overexpression of the Cx32 gene was verified with qRT-PCR. For both cell types, the Cx32 mRNA levels were normalized to Cx32 mRNA levels of control cells (infected with pLenti GFP). The mRNA levels for Cx32 increased approximately two hundred-folds for MDA-MB-231 pLenti-Cx32-GFP (p< 0.01 ***, n=2) and approximately a hundred-fold for MCF10A pLenti-Cx32-GFP cells compared to pLenti-GFP cells as a result of infection.

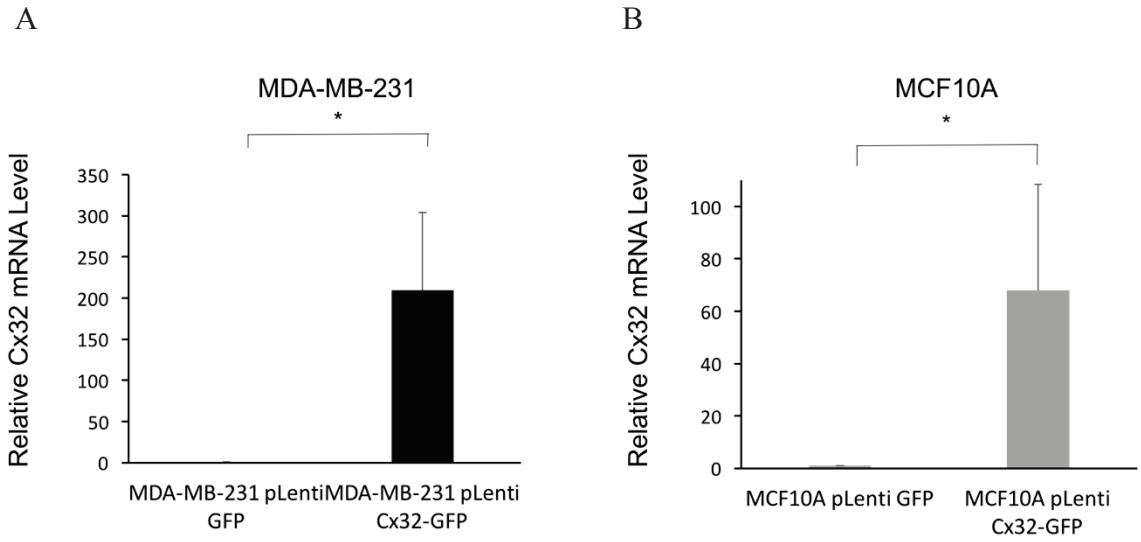

Figure 3. 3. Relative Cx32 mRNA levels of MDA-MB-231 and MCF10A cells infected with pLenti-GFP or pLenti-Cx32-EGFP vectors. A) Relative Cx32 mRNA levels of MDA-MB-231 cells (n=3) B) Relative Cx32 mRNA levels of MCF10A cells (n=3). They were normalized to Cx32 mRNA levels of MDA-MB-231 pLenti GFP and MCF10A pLenti respectively (p< 0.05 *).

3.4. Gap Junction Coupling in MDA-MB-231 and MCF10A cells

Connexins can form hemichannels and/or gap junctions on the plasma membrane in addition to localization in the cytoplasm. After stable cell lines were generated in MDA-MB-231 (Figure 3.4 and 3.5) and MCF10A (Figure 3.6 and 3.7) cells with the infection of pLenti GFP and pLenti Cx32-GFP vectors, the difference in the gap junction coupling was assessed with scrape loading assay to see if the overexpressed Cx32 results in the formation of gap junctions. In these experiments, carbenoxolone (CBX), a gap junction/hemichannel blocker, was used as a negative control [72]. In MDA-MB-231 cells the overexpression of Cx32 did not alter gap junction coupling when it is compared to control cells (n=1, Figure 3.5). However, in MCF10A cells, Cx32 overexpression increased the gap junctional coupling of MCF10A pLenti Cx32-GFP cells compared to uninfected cells by 29 %, which was significant statically ($p < 0.01$, n=2, Figure 3.7).

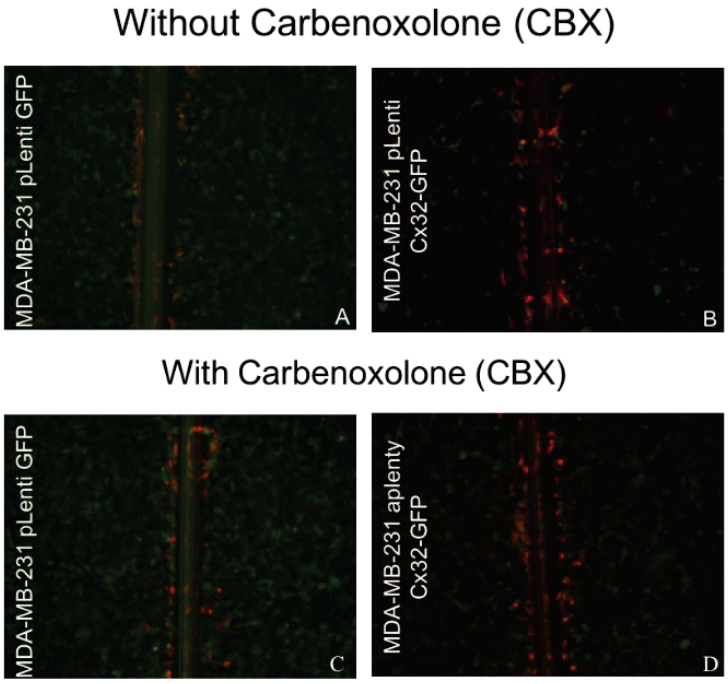

Figure 3. 4. Merged images of scrape loading results of MDA-MB-231 stable cells. In absence of CBX, A) MDA-MB-231 pLenti GFP cells B) MDA-MB-231 pLenti Cx32-GFP cells; In the presence of CBX, C) MDA-MB-231 pLenti GFP cells D) MDA-MB-231 pLenti Cx32-GFP cells. Red color represents NB, green color represents GFP.

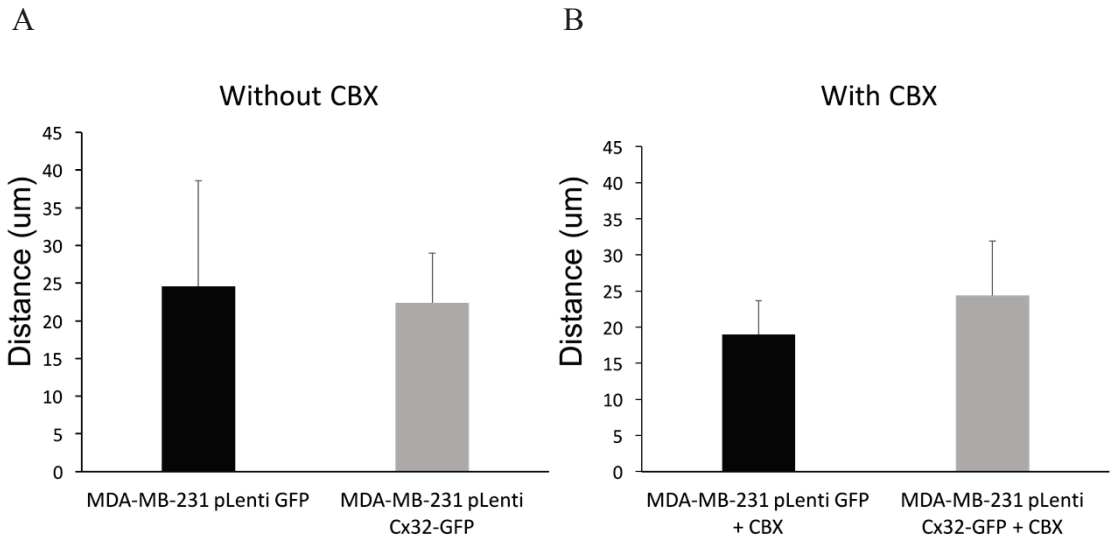

Figure 3. 5. Comparison of distance of NB signaling from the scrape in MDA-MB-231 stable cells (n=1, 10 images were analyzed for each group).

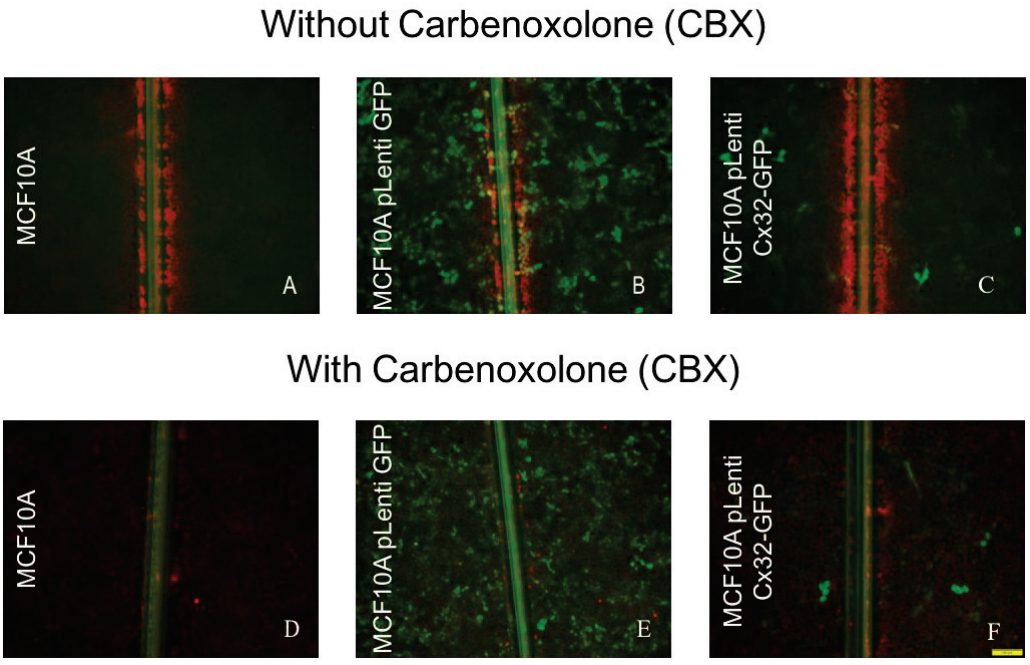

Figure 3. 6. Merged images of scrape loading results of MCF10A and MCF10A stable cells. In absence of CBX, A) MCF10A cells B) MCF10A pLenti GFP cells C) MCF10A pLenti Cx32-GFP cells; In the presence of CBX, D) MCF10A cells E) MCF10A pLenti GFP cells D) MCF10A pLenti Cx32-GFP cells. Red color represents NB, green color represents GFP.

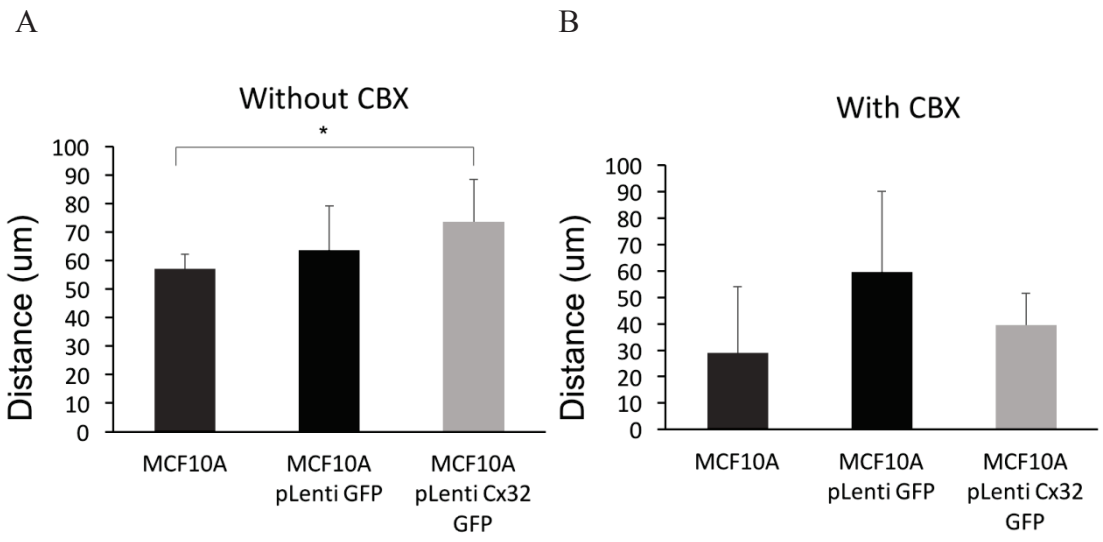

Figure 3. 7. Comparison of distance of NB signaling from the scrape in MCF10A cells. A) Gap junction coupling in MCF10A cells (n=2, p< 0.01 ***) B) Gap junction coupling in MCF10A cells with CBX (n=1, 4 images were analyzed for each group).

3.5. Hemichannel Activities in MDA-MB-231 and MCF10A cells

In order to determine if Cx32 overexpression results in functional hemichannels in the plasma membrane, dye uptake assay was performed for both MDA-MB-231 (Figure 3.8 and 3.9) and MCF10A (Figure 3.10 and 3.11) cells. The neurobiotin uptake analysis with the Image J program demonstrated that the Cx32 overexpression did not result in functional hemichannels for both cell types (Figure 3.9 and Figure 3.11, n=1).

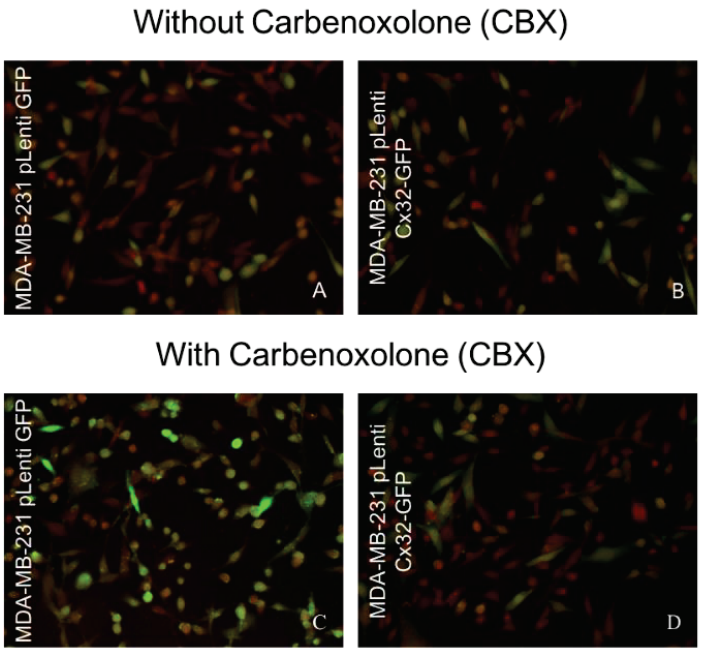

Figure 3. 8. Merged images of dye uptake results of MDA-MB-231 stable cells. In absence of CBX, A) MDA-MB-231 pLenti GFP cells B) MDA-MB-231 pLenti Cx32-GFP cells; In the presence of CBX, C) MDA-MB-231 pLenti GFP cells D) MDA-MB-231 pLenti Cx32-GFP cells. Red color represents NB taken by the cells, green color represents GFP producing cells.

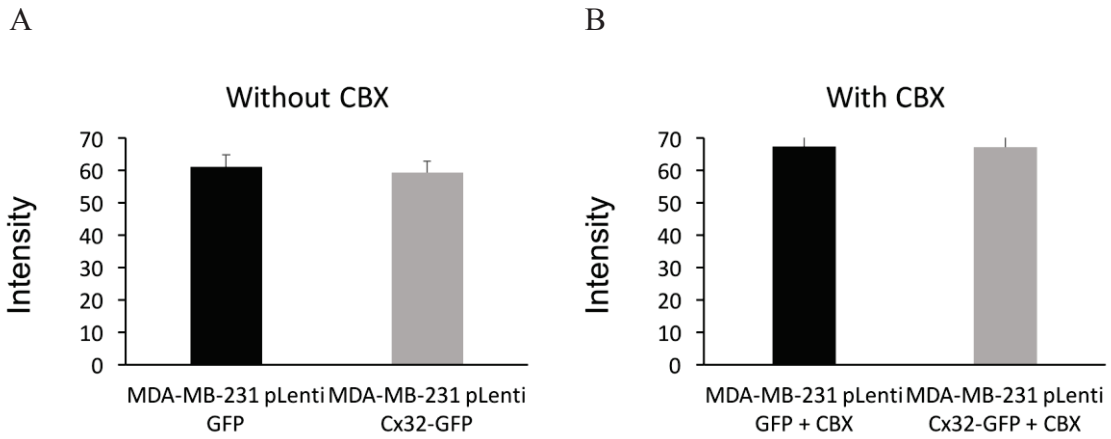

Figure 3. 9. Comparison of NB uptake in MDA-MB-231 stable cells (n=1, 10 images were analyzed for each group).

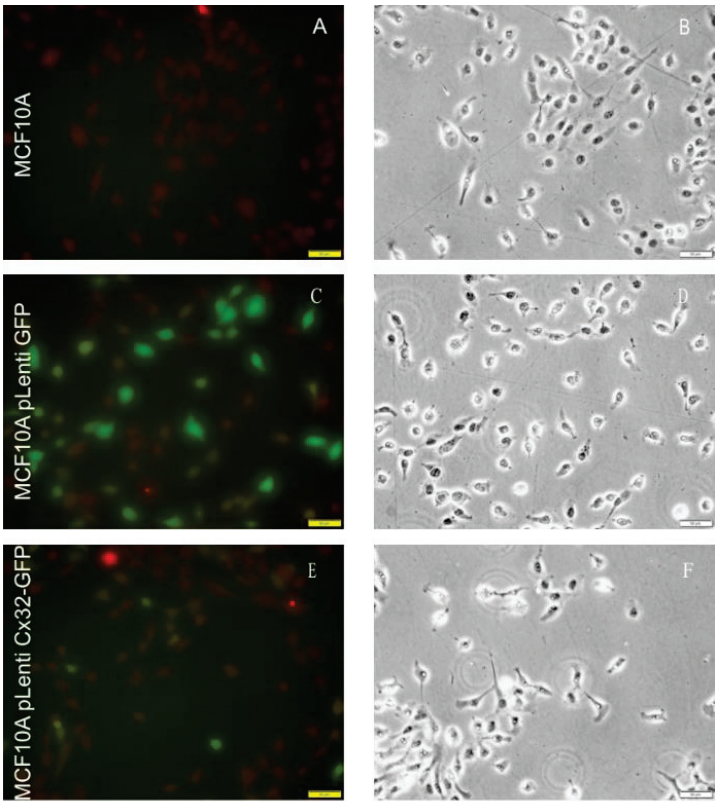

Figure 3. 10. Merged images of dye uptake results of MCF10A and MCF10A stable cells. A, B) MCF10A cells C, D) MCF10A pLenti GFP cells E, F) MCF10A pLenti Cx32-GFP cells. A, C and E are merged images of GFP and Alexa 555 red signal; B, D and F are phase contrast images of A, C and E respectively. Red color represents NB taken by the cells, green color represents GFP producing cells.

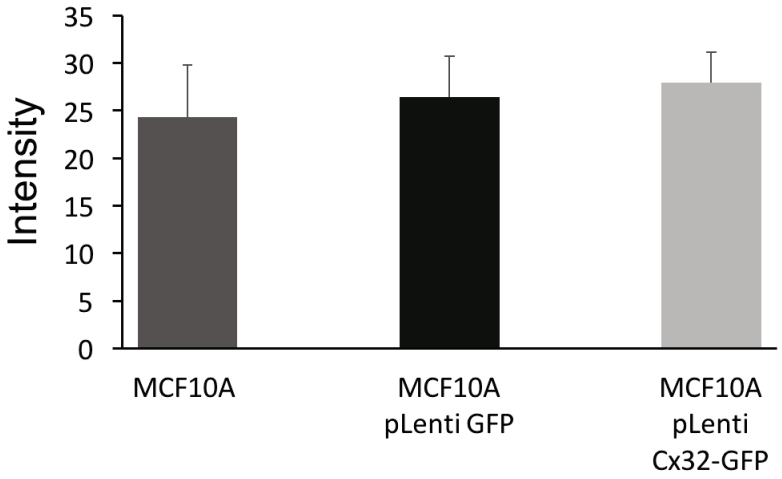

Figure 3. 11. Comparison of NB uptake in MCF10A cells (n=1, 4 images were analyzed for each group).

3.6. Cell Viability Assessments in MDA-MB-231 and MCF10A cells

In order to see how Cx32 overexpression affect the cell proliferation, cell viability of MDA-MB-231 and MCF10A stable cells were assessed with MTT Assay. The cells' absorbance values were measured with spectrophotometer on Day 1, Day 4, Day 7 and Day 10. Overexpression led to an increase in cell viability of MDA-MB-231 cells (Figure 3.12 A), but it was not statically significant (n=2). However, overexpression of Cx32 resulted in a decrease by 27.4 % on day 4, 42.8 % on day 7 and 37.9 % on day 10 in cell viability of MCF10A cells significantly (n=2, $p<0.05$ *, $p< 0.01$ ***, Figure 3.12 B).

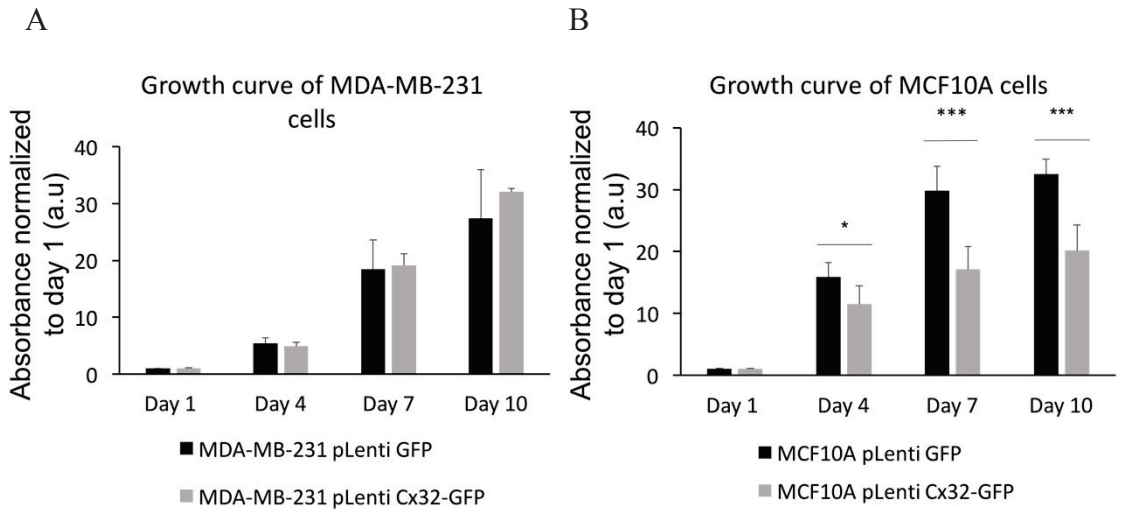

Figure 3. 12. Growth curves of MDA-MB-231 and MCF10A stable cells. A) Growth curve of MDA-MB-231 cells (n=2), B) Growth curve of MCF10A cells (n=2, $p<0.05$ *, $p< 0.01$ ***).

3.7. Cell Cycle Assessments in MDA-MB-231 and MCF10A cells

Connexins affect cell cycle either by junctional or non-junctional ways. These could be mediated by interacting with proteins regarding to cell proliferation in cytoplasm or on the plasma membrane. Connexins can directly affect gene transcription. In addition to these the molecules passing through hemichannels and gap junctions can cause modulation of gene transcription related to cell proliferation [73]. Based on these, in

order to understand how Cx32 overexpression affects the cell cycle profiles of the cells, PI staining with flow cytometer was performed. As it is observed in Figure 3.13, percentage of cells in G_2 level increased by 2.32 whereas percentage of cells in G_1 cycle decreased by 4.2 with the overexpression of Cx32 in MDA-MB-231 cells compared to MDA-MB-231 pLenti GFP (n=2, p< 0,05 *, p< 0.01 ***). However, the change in S phase was not statically significant. In MCF10A cells when Cx32 was overexpressed it led to an increase in G_2, a decrease in S phase, which were not significant in terms of statistical analysis (n=2).

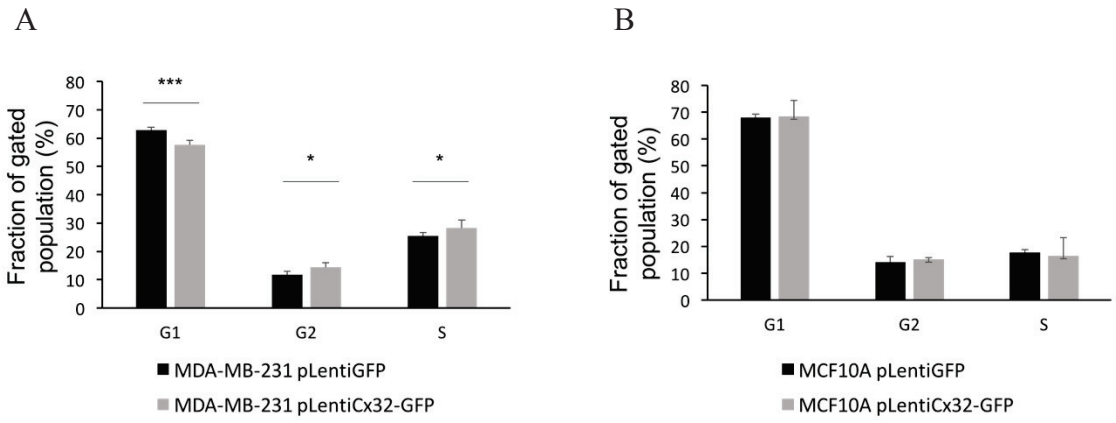

Figure 3. 13. Cell cycle assessment showing fraction of gated population of MDA-MB-231 and MCF10A stable cells. A) Cell cycle assessment of MDA-MB-231 cells (n=3, p< 0,05 *, p< 0.01 ***) B) Cell cycle assessment of MCF10A cells (n=2).

CHAPTER 4

DISCUSSION AND CONCLUSION

As it is indicated before, Cx32 was found in normal pre-menopausal breast tissue and tumor samples obtained from patients [70]. In addition to this, when Cx32 expression was compared in primary breast cancer and its lymph node metastasis, the level was seen to increase in metastasis [71]. Therefore, it was hypothesized that Cx32 may play a role in breast cancer initiation and/or progression. To verify this hypothesis, Cx32 was overexpressed in MDA-MB-231 and MCF10A cells. In the first place the overexpression was performed transiently with transfection of pIRES2-EGFP2 vectors. This was confirmed with immunostaining and qRT-PCR methods. As a result of immunostaining, Cx32 protein was observed to increase in both MDA-MB-231 and MCF10A transfected with pIRES2-Cx32-EGFP2 compared to untransfected or pIRES2-EGFP2 transfected cells. In addition to this, in MCF10A transfected with pIRES2-Cx32-EGFP2, Cx32 formed gap junctional plaques in the cell membrane between adjacent cells. As a result of qRT-PCR, mRNA levels of Cx32 increased significantly in MDA-MB-231 transfected with Cx32 compared to untransfected cells ($p< 0.01$, $n=2$). The increase in Cx32 mRNA level of Cx32 transfected MCF10A was not statically significant ($n=2$). Since the transfection was not very efficient, stable cell lines overexpressing Cx32 were generated. The overexpression of Cx32 was verified with qRT-PCR where the relative mRNA levels of Cx32 infected cells significantly increased for MDA-MB-231 and MCF10A ($n=3$ $p>0.05$). When it comes to questions of what these overexpressed Cx32 proteins do in the cell and if they form channels on the plasma membrane, the gap junctional coupling of the cells and their hemichannels activity were controlled. For gap junction coupling assessment, scrape loading experiment was performed. In MDA-MB-231 cells the gap junctional coupling did not change with overexpression of Cx32 ($n=1$) while in MC10A cells however, the gap junctional coupling increased with overexpressing Cx32 ($n=2$, $p< 0.01$). For the hemichannels activity assessment, dye uptake was performed. In this experiment, the Cx32 overexpressing cells' hemichannels activities and control groups' activities were compared. There was no difference between Cx32 infected and their control groups in

both MDA-MB-231 and MCF10A cells (n=1). MDA-MB-231 overexpressing Cx32 proliferated more but the difference was not significant statistically (n=2). MCF10A overexpressing Cx32 however, proliferated less on day 4, 7 and 10 significantly (n=2, $p<0.05$, $p< 0.01$). In cell cycle analysis, G_1 phase decreased whereas S and G_2 phases increased in MDA-MB-231 overexpressing Cx32 significantly (n=3, $p< 0,05$, $p< 0.01$). In MCF10A cells however, the cell cycle did not change significantly (n=2).

In this study, the Cx32 overexpressing cells' gap junctional coupling and control groups' coupling were compared. As it is seen with the results of analysis, the overexpression of Cx32 did not lead to an increase in MDA-MB-231 cell gap junctional coupling. This is possible since the proteins can locate in cytoplasm or nucleus inside the cells and can have different function rather than forming gap junctions as it is shown with C terminal of Cx43 transfection. They showed that to be able to be functional, connexins do not have to localize in the membrane but they can localize in nucleus and cytoplasm [74]. This could also be caused by experimental problems because MDA-MB-231 cells were detaching from the surface during experiment. As a result, analysis of the images could not be done properly. In MCF10A cells however, the overexpression of Cx32 led to an increase in gap junctional coupling, which means the Cx32 expressed in the cells participate into gap junctions on the membrane in MCF10A cells.

The overexpression of Cx32 did not result in change in the hemichannel activity. This is one of the possibility that is expected because connexins do not have to be active in form of hemichannels. As Thimm et al. (2005) suggested, in mammalian tissues, non-junctional connexons (formed by Cx43, Cx26 and Cx32) are generally inactive to prevent uncontrolled molecule exchange across the plasma membrane [75].

Once the effect of Cx32 overexpression on proliferation was controlled it was seen that Cx32 overexpressing MDA-MB-231 cells are more viable compared to control cells but the error bars were high, therefore it was not significant and this experiment should be repeated. For MCF10A overexpressing Cx32 protein however, the increase in Cx32 expression led to a decrease in cell viability (Figure 3.12 B). The increase in gap junctional coupling might have led to this decrease in MCF10A cells. It was previously shown that the growth of the transfected cells was observed to decrease when Cx43 was overexpressed in C6 glioma cells [76]. This means, connexin overexpression can alter the cell proliferation.

In the last part of the study, PI staining was performed in order to assess the change in the cell cycle profile in Cx32 overexpressed cells. G_2 and S levels increased

while G_1 cycle decreased in MDA-MB-231 pLenti-Cx32-GFP cells compared to in MDA-MB-231 pLenti-GFP cells. The changes in G_1, S and G_2 levels were significant between control and Cx32 overexpressing cells (n=2, p< 0,05, p< 0.01). Cx26 expression was shown to lead to G_2 arrest in PC-3, LNCap, and DU-145 (human prostate cancer cell lines) [77], therefore the overexpression of Cx32 in MDA-MB-231 cells can cause a similar effect and result in G_2 arrest in a context dependent manner. In MCF10A cells, when Cx32 was overexpressed, it led to an increase in G2, \ decrease in S cycle but they were not statistically significant.

When rat Cx43 gene was transfected into TRMP cell line, the duration of S phase was doubled and the cell growth was decreased [78], which indicated that change in the S phase can affect the cell growth. Therefore, the change in the growth of MDA-MB-231 and MCF10A cells overexpressing Cx32 can be linked to their change in S phase although the increase in cell growth of MDA-MB-231 and the change in S phase of MCF10A cells were not significant.

For the further assessment of Cx32 role in progression of breast cancer, migration and invasion assays can be performed. In the end, determination of the differential role of Cx32 in different stages of breast cancer development may help us to understand its diagnostic and/or therapeutic potential.

REFERENCES

1. Mese, G.; Richard, G.; White, T. W., Gap junctions: basic structure and function. *J Invest Dermatol* 2007, *127* (11), 2516-24.

2. Qin, H.; Shao, Q.; Igdoura, S. A.; Alaoui-Jamali, M. A.; Laird, D. W., Lysosomal and proteasomal degradation play distinct roles in the life cycle of Cx43 in gap junctional intercellular communication-deficient and -competent breast tumor cells. *J Biol Chem* 2003, *278* (32), 30005-14.

3. Evans, W. H.; Martin, P. E., Gap junctions: structure and function (Review). *Mol Membr Biol* 2002, *19* (2), 121-36.

4. Goodenough, D. A.; Paul, D. L., Gap junctions. *Cold Spring Harb Perspect Biol* 2009, *1* (1), a002576.

5. Dbouk, H. A.; Mroue, R. M.; El-Sabban, M. E.; Talhouk, R. S., Connexins: a myriad of functions extending beyond assembly of gap junction channels. *Cell Commun Signal* 2009, *7*, 4.

6. Burra, S.; Jiang, J. X., Regulation of cellular function by connexin hemichannels. *Int J Biochem Mol Biol* 2011, *2* (2), 119-128.

7. Evans, W. H.; De Vuyst, E.; Leybaert, L., The gap junction cellular internet: connexin hemichannels enter the signalling limelight. *Biochem J* 2006, *397* (1), 1-14.

8. Plotkin, L. I.; Manolagas, S. C.; Bellido, T., Transduction of cell survival signals by connexin-43 hemichannels. *J Biol Chem* 2002, *277* (10), 8648-57.

9. Saez, J. C.; Contreras, J. E.; Bukauskas, F. F.; Retamal, M. A.; Bennett, M. V., Gap junction hemichannels in astrocytes of the CNS. *Acta Physiol Scand* 2003, *179* (1), 9-22.

10. Panchin, Y. V., Evolution of gap junction proteins--the pannexin alternative. *J Exp Biol* 2005, *208* (Pt 8), 1415-9.

11. Goodenough, D. A., Bulk isolation of mouse hepatocyte gap junctions. Characterization of the principal protein, connexin. *J Cell Biol* 1974, *61* (2), 557-63.

12. Barbe, M. T.; Monyer, H.; Bruzzone, R., Cell-cell communication beyond connexins: the pannexin channels. *Physiology (Bethesda)* 2006, *21*, 103-14.

13. Laird, D. W., Life cycle of connexins in health and disease. *Biochem J* 2006, *394* (Pt 3), 527-43.

14. Zonta, F.; Polles, G.; Zanotti, G.; Mammano, F., Permeation pathway of homomeric connexin 26 and connexin 30 channels investigated by molecular dynamics. *J Biomol Struct Dyn* 2012, *29* (5), 985-98.

15. Sohl, G.; Willecke, K., Gap junctions and the connexin protein family. *Cardiovasc Res* 2004, *62* (2), 228-32.

16. Mathias, R. T.; White, T. W.; Gong, X., Lens gap junctions in growth, differentiation, and homeostasis. *Physiol Rev* 2010, *90* (1), 179-206.

17. Sosinsky, G., Mixing of connexins in gap junction membrane channels. *Proc Natl Acad Sci U S A* 1995, *92* (20), 9210-4.

18. Hopperstad, M. G.; Srinivas, M.; Spray, D. C., Properties of gap junction channels formed by Cx46 alone and in combination with Cx50. *Biophys J* 2000, *79* (4), 1954-66.

19. Jiang, J. X.; Goodenough, D. A., Heteromeric connexons in lens gap junction channels. *Proc Natl Acad Sci U S A* 1996, *93* (3), 1287-91.

20. Sun, J.; Ahmad, S.; Chen, S.; Tang, W.; Zhang, Y.; Chen, P.; Lin, X., Cochlear gap junctions coassembled from Cx26 and 30 show faster intercellular Ca2+ signaling than homomeric counterparts. *Am J Physiol Cell Physiol* 2005, *288* (3), C613-23.

21. Srinivas, M.; Verselis, V. K.; White, T. W., Human diseases associated with connexin mutations. *Biochim Biophys Acta* 2017.

22. Goldberg, G. S.; Valiunas, V.; Brink, P. R., Selective permeability of gap junction channels. *Biochim Biophys Acta* 2004, *1662* (1-2), 96-101.

23. Volgyi, B.; Kovacs-Oller, T.; Atlasz, T.; Wilhelm, M.; Gabriel, R., Gap junctional coupling in the vertebrate retina: variations on one theme? *Prog Retin Eye Res* 2013, *34*, 1-18.

24. Koval, M., Pathways and control of connexin oligomerization. *Trends Cell Biol* 2006, *16* (3), 159-66.

25. Zhang, J. T.; Chen, M.; Foote, C. I.; Nicholson, B. J., Membrane integration of in vitro-translated gap junctional proteins: co- and post-translational mechanisms. *Mol Biol Cell* 1996, *7* (3), 471-82.

26. Musil, L. S.; Goodenough, D. A., Multisubunit assembly of an integral plasma membrane channel protein, gap junction connexin43, occurs after exit from the ER. *Cell* 1993, *74* (6), 1065-77.

27. Evans, W. H.; Ahmad, S.; Diez, J.; George, C. H.; Kendall, J. M.; Martin, P. E., Trafficking pathways leading to the formation of gap junctions. *Novartis Found Symp* 1999, *219*, 44-54; discussion 54-9.

28. Lauf, U.; Giepmans, B. N.; Lopez, P.; Braconnot, S.; Chen, S. C.; Falk, M. M., Dynamic trafficking and delivery of connexons to the plasma membrane and accretion to gap junctions in living cells. *Proc Natl Acad Sci U S A* 2002, *99* (16), 10446-51.

29. Evans, W. H., Cell communication across gap junctions: a historical perspective and current developments. *Biochem Soc Trans* 2015, *43* (3), 450-9.

30. Nielsen, M. S.; Axelsen, L. N.; Sorgen, P. L.; Verma, V.; Delmar, M.; Holstein-Rathlou, N. H., Gap junctions. *Compr Physiol* 2012, *2* (3), 1981-2035.

31. Rackauskas, M.; Neverauskas, V.; Skeberdis, V. A., Diversity and properties of connexin gap junction channels. *Medicina (Kaunas)* 2010, *46* (1), 1-12.

32. Bukauskas, F. F.; Verselis, V. K., Gap junction channel gating. *Biochim Biophys Acta* 2004, *1662* (1-2), 42-60.

33. Liu, G. N.; Guo, G. C.; Chen, F.; Wang, S. H.; Sun, J.; Huang, J. S., Structural diversity, optical and magnetic properties of a series of manganese thioarsenates with 1,10-phenanthroline or 2,2'-bipyridine ligands: using monodentate methylamine as an alkalinity regulator. *Inorg Chem* 2012, *51* (1), 472-82.

34. Palacios-Prado, N.; Sonntag, S.; Skeberdis, V. A.; Willecke, K.; Bukauskas, F. F., Gating, permselectivity and pH-dependent modulation of channels formed by connexin57, a major connexin of horizontal cells in the mouse retina. *J Physiol* 2009, *587* (Pt 13), 3251-69.

35. Gonzalez-Nieto, D.; Gomez-Hernandez, J. M.; Larrosa, B.; Gutierrez, C.; Munoz, M. D.; Fasciani, I.; O'Brien, J.; Zappala, A.; Cicirata, F.; Barrio, L. C., Regulation of neuronal connexin-36 channels by pH. *Proc Natl Acad Sci U S A* 2008, *105* (44), 17169-74.

36. Urschel, S.; Hoher, T.; Schubert, T.; Alev, C.; Sohl, G.; Worsdorfer, P.; Asahara, T.; Dermietzel, R.; Weiler, R.; Willecke, K., Protein kinase A-mediated phosphorylation of connexin36 in mouse retina results in decreased gap junctional communication between AII amacrine cells. *J Biol Chem* 2006, *281* (44), 33163-71.

37. Ngezahayo, A.; Zeilinger, C.; Todt, I.; Marten, I.; Kolb, H. A., Inactivation of expressed and conducting rCx46 hemichannels by phosphorylation. *Pflugers Arch* 1998, *436* (4), 627-9.

38. Jani-Acsadi, A.; Ounpuu, S.; Pierz, K.; Acsadi, G., Pediatric Charcot-Marie-Tooth disease. *Pediatr Clin North Am* 2015, *62* (3), 767-86.

39. Beyer, E. C.; Ebihara, L.; Berthoud, V. M., Connexin mutants and cataracts. *Front Pharmacol* 2013, *4*, 43.

40. Kelsell, D. P.; Di, W. L.; Houseman, M. J., Connexin mutations in skin disease and hearing loss. *Am J Hum Genet* 2001, *68* (3), 559-68.

41. Aasen, T.; Mesnil, M.; Naus, C. C.; Lampe, P. D.; Laird, D. W., Gap junctions and cancer: communicating for 50 years. *Nat Rev Cancer* 2016, *16* (12), 775-788.

42. Mesnil, M.; Crespin, S.; Avanzo, J. L.; Zaidan-Dagli, M. L., Defective gap junctional intercellular communication in the carcinogenic process. *Biochim Biophys Acta* 2005, *1719* (1-2), 125-45.

43. Laird, D. W., The gap junction proteome and its relationship to disease. *Trends Cell Biol* 2010, *20* (2), 92-101.

44. McLachlan, E.; Shao, Q.; Laird, D. W., Connexins and gap junctions in mammary gland development and breast cancer progression. *J Membr Biol* 2007, *218* (1-3), 107-21.

45. Lee, S. W.; Tomasetto, C.; Sager, R., Positive selection of candidate tumor-suppressor genes by subtractive hybridization. *Proc Natl Acad Sci U S A* 1991, *88* (7), 2825-9.

46. Wilgenbus, K. K.; Kirkpatrick, C. J.; Knuechel, R.; Willecke, K.; Traub, O., Expression of Cx26, Cx32 and Cx43 gap junction proteins in normal and neoplastic human tissues. *Int J Cancer* 1992, *51* (4), 522-9.

47. Pozzi, A.; Risek, B.; Kiang, D. T.; Gilula, N. B.; Kumar, N. M., Analysis of multiple gap junction gene products in the rodent and human mammary gland. *Exp Cell Res* 1995, *220* (1), 212-9.

48. Laird, D. W.; Fistouris, P.; Batist, G.; Alpert, L.; Huynh, H. T.; Carystinos, G. D.; Alaoui-Jamali, M. A., Deficiency of connexin43 gap junctions is an independent marker for breast tumors. *Cancer Res* 1999, *59* (16), 4104-10.

49. Monaghan, P.; Clarke, C.; Perusinghe, N. P.; Moss, D. W.; Chen, X. Y.; Evans, W. H., Gap junction distribution and connexin expression in human breast. *Exp Cell Res* 1996, *223* (1), 29-38.

50. Locke, D.; Jamieson, S.; Stein, T.; Liu, J.; Hodgins, M. B.; Harris, A. L.; Gusterson, B., Nature of Cx30-containing channels in the adult mouse mammary gland. *Cell Tissue Res* 2007, *328* (1), 97-107.

51. Locke, D.; Perusinghe, N.; Newman, T.; Jayatilake, H.; Evans, W. H.; Monaghan, P., Developmental expression and assembly of connexins into homomeric and heteromeric gap junction hemichannels in the mouse mammary gland. *J Cell Physiol* 2000, *183* (2), 228-37.

52. Locke, D.; Stein, T.; Davies, C.; Morris, J.; Harris, A. L.; Evans, W. H.; Monaghan, P.; Gusterson, B., Altered permeability and modulatory character of connexin channels during mammary gland development. *Exp Cell Res* 2004, *298* (2), 643-60.

53. Talhouk, R. S.; Elble, R. C.; Bassam, R.; Daher, M.; Sfeir, A.; Mosleh, L. A.; El-Khoury, H.; Hamoui, S.; Pauli, B. U.; El-Sabban, M. E., Developmental expression patterns and regulation of connexins in the mouse mammary gland: expression of connexin30 in lactogenesis. *Cell Tissue Res* 2005, *319* (1), 49-59.

54. Monaghan, P.; Perusinghe, N.; Carlile, G.; Evans, W. H., Rapid modulation of gap junction expression in mouse mammary gland during pregnancy, lactation, and involution. *J Histochem Cytochem* 1994, *42* (7), 931-8.

55. Lambe, T.; Finlay, D.; Murphy, M.; Martin, F., Differential expression of connexin 43 in mouse mammary cells. *Cell Biol Int* 2006, *30* (5), 472-9.

56. Jemal, A.; Bray, F.; Center, M. M.; Ferlay, J.; Ward, E.; Forman, D., Global cancer statistics. *CA Cancer J Clin* 2011, *61* (2), 69-90.

57. Naus, C. C.; Laird, D. W., Implications and challenges of connexin connections to cancer. *Nat Rev Cancer* 2010, *10* (6), 435-41.

58. Lee, S. W.; Tomasetto, C.; Paul, D.; Keyomarsi, K.; Sager, R., Transcriptional downregulation of gap-junction proteins blocks junctional communication in human mammary tumor cell lines. *J Cell Biol* 1992, *118* (5), 1213-21.

59. Jamieson, S.; Going, J. J.; D'Arcy, R.; George, W. D., Expression of gap junction proteins connexin 26 and connexin 43 in normal human breast and in breast tumours. *J Pathol* 1998, *184* (1), 37-43.

60. Hirschi, K. K.; Xu, C. E.; Tsukamoto, T.; Sager, R., Gap junction genes Cx26 and Cx43 individually suppress the cancer phenotype of human mammary carcinoma cells and restore differentiation potential. *Cell Growth Differ* 1996, *7* (7), 861-70.

61. Qin, H.; Shao, Q.; Curtis, H.; Galipeau, J.; Belliveau, D. J.; Wang, T.; Alaoui-Jamali, M. A.; Laird, D. W., Retroviral delivery of connexin genes to human breast tumor cells inhibits in vivo tumor growth by a mechanism that is independent of significant gap junctional intercellular communication. *J Biol Chem* 2002, *277* (32), 29132-8.

62. McLachlan, E.; Shao, Q.; Wang, H. L.; Langlois, S.; Laird, D. W., Connexins act as tumor suppressors in three-dimensional mammary cell organoids by regulating differentiation and angiogenesis. *Cancer Res* 2006, *66* (20), 9886-94.

63. Shao, Q.; Wang, H.; McLachlan, E.; Veitch, G. I.; Laird, D. W., Down-regulation of Cx43 by retroviral delivery of small interfering RNA promotes an aggressive breast cancer cell phenotype. *Cancer Res* 2005, *65* (7), 2705-11.

64. Kanczuga-Koda, L.; Sulkowski, S.; Lenczewski, A.; Koda, M.; Wincewicz, A.; Baltaziak, M.; Sulkowska, M., Increased expression of connexins 26 and 43 in lymph node metastases of breast cancer. *J Clin Pathol* 2006, *59* (4), 429-33.

65. Bellahcene, A.; Bachelier, R.; Detry, C.; Lidereau, R.; Clezardin, P.; Castronovo, V., Transcriptome analysis reveals an osteoblast-like phenotype for human osteotropic breast cancer cells. *Breast Cancer Res Treat* 2007, *101* (2), 135-48.

66. Li, Q.; Omori, Y.; Nishikawa, Y.; Yoshioka, T.; Yamamoto, Y.; Enomoto, K., Cytoplasmic accumulation of connexin32 protein enhances motility and metastatic ability of human hepatoma cells in vitro and in vivo. *Int J Cancer* 2007, *121* (3), 536-46.

67. Zhao, B.; Zhao, W.; Wang, Y.; Xu, Y.; Xu, J.; Tang, K.; Zhang, S.; Yin, Z.; Wu, Q.; Wang, X., Connexin32 regulates hepatoma cell metastasis and proliferation via the p53 and Akt pathways. *Oncotarget* 2015, *6* (12), 10116-33.

68. Yang, Y.; Zhang, N.; Zhu, J.; Hong, X. T.; Liu, H.; Ou, Y. R.; Su, F.; Wang, R.; Li, Y. M.; Wu, Q., Downregulated connexin32 promotes EMT through the Wnt/beta-catenin pathway by targeting Snail expression in hepatocellular carcinoma. *Int J Oncol* 2017, *50* (6), 1977-1988.

69. Nakashima, Y.; Ono, T.; Yamanoi, A.; El-Assal, O. N.; Kohno, H.; Nagasue, N., Expression of gap junction protein connexin32 in chronic hepatitis, liver cirrhosis, and hepatocellular carcinoma. *J Gastroenterol* 2004, *39* (8), 763-8.

70. Teleki, I.; Szasz, A. M.; Maros, M. E.; Gyorffy, B.; Kulka, J.; Meggyeshazi, N.; Kiszner, G.; Balla, P.; Samu, A.; Krenacs, T., Correlations of differentially expressed gap junction connexins Cx26, Cx30, Cx32, Cx43 and Cx46 with breast cancer progression and prognosis. *PLoS One* 2014, *9* (11), e112541.

71. Kanczuga-Koda, L.; Sulkowska, M.; Koda, M.; Rutkowski, R.; Sulkowski, S., Increased expression of gap junction protein--connexin 32 in lymph node metastases of human ductal breast cancer. *Folia Histochem Cytobiol* 2007, *45 Suppl 1*, S175-80.

72. Ozog, M. A.; Siushansian, R.; Naus, C. C., Blocked gap junctional coupling increases glutamate-induced neurotoxicity in neuron-astrocyte co-cultures. *J Neuropathol Exp Neurol* 2002, *61* (2), 132-41.

73. Aasen, T., Connexins: junctional and non-junctional modulators of proliferation. *Cell Tissue Res* 2015, *360* (3), 685-99.

74. Dang, X.; Doble, B. W.; Kardami, E., The carboxy-tail of connexin-43 localizes to the nucleus and inhibits cell growth. *Mol Cell Biochem* 2003, *242* (1-2), 35-8.

75. Thimm, J.; Mechler, A.; Lin, H.; Rhee, S.; Lal, R., Calcium-dependent open/closed conformations and interfacial energy maps of reconstituted hemichannels. *J Biol Chem* 2005, *280* (11), 10646-54.

76. Zhu, D.; Kidder, G. M.; Caveney, S.; Naus, C. C., Growth retardation in glioma cells cocultured with cells overexpressing a gap junction protein. *Proc Natl Acad Sci U S A* 1992, *89* (21), 10218-21.

77. Tanaka, M.; Grossman, H. B., Connexin 26 induces growth suppression, apoptosis and increased efficacy of doxorubicin in prostate cancer cells. *Oncol Rep* 2004, *11* (2), 537-41.

78. Chen, S. C.; Pelletier, D. B.; Ao, P.; Boynton, A. L., Connexin43 reverses the phenotype of transformed cells and alters their expression of cyclin/cyclin-dependent kinases. *Cell Growth Differ* 1995, *6* (6), 681-90.